Agricultural and Forest Meteorology 300 (2021) 108310

Contents lists available at ScienceDirect

Agricultural and Forest Meteorology

journal homepage: www.elsevier.com/locate/agrformet

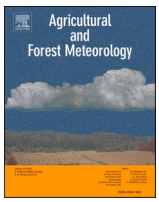

Solar energy dominates and soil water modulates net ecosystem productivity and evapotranspiration across multiple timescales in a subtropical coniferous plantation

Yakun Tang [a], Chang Jia [a], Lina Wang [a], Xuefa Wen [b,*], Huimin Wang [b]

[a] State Key Laboratory of Soil Erosion and Dryland Farming on the Loess Plateau, Northwest A&F University, Yangling, 712100, China
[b] Key Laboratory of Ecosystem Network Observation and Modeling, Institute of Geographic Sciences and Natural Resources Research, Chinese Academy of Sciences, Beijing 100101, China

ARTICLE INFO

Keywords:
Coniferous plantation
Eddy covariance
ET
NEP
Wavelet analysis

ABSTRACT

The timescale dependence of environmental factors' influence on net ecosystem productivity (NEP), evapotranspiration (ET), and the effect of high and cool air temperature (Ta) across multiple timescales need to be quantified to identify the response mechanisms of forest ecosystems. We analyzed NEP and ET over 11 years in a subtropical coniferous plantation, and wavelet analysis was used to determine spectrum characteristics of these fluxes and quantify the time lag between these fluxes and environmental factors from daily to annual timescales. The NEP and ET had significant daily and annual spectrum variabilities, but ET exhibited a broader significant spectrum than NEP from days to months timescales. At daily and annual timescales, NEP was significantly synchronized with, and preceded photosynthetically active radiation (PAR) and Ta by 1. 12 ± 0.6 h and 23.16 ± 17 days, respectively. Meanwhile, ET was significantly synchronized with net radiation (Rn) at both daily and annual timescales, lagging Rn by 1.15 ± 1.4 h, but preceding it by 5. 73 ± 4.39 days, respectively. From days to months timescales, with no continuous significant effect, NEP preceded PAR and vapor pressure deficit (VPD), and lagged soil water content (SW); however, ET only preceded Rn and VPD. In addition, summer high-Ta enhanced the effect of SW on NEP and ET across multiple timescales. Early spring cool-Ta shortened the time lag between PAR and NEP at daily and annual timescales, but only shortened it between Ta and ET at a daily timescale. This study demonstrated the more modulating effect of SW on the dominant influence of solar energy on NEP than ET, with timescale increased. This study also indicated that NEP and ET were more sensitive to high- than cool-Ta, and the time lag effects of these Ta events should be considered separately to adequately acknowledge the response mechanisms of these fluxes.

1. Introduction

Forests occupy more than one-third of the terrestrial area, and play an essential role in the carbon and water cycles between the land surface and atmosphere (Baldocchi et al., 2000; Wilson et al., 2002; Tian et al., 2020). High and cool air temperature (Ta) events may frequently occur in terms of changing climatic conditions and, along with other environmental factors, influence carbon and water flux variations (Baldocchi et al., 2018; Hu et al., 2018). Ecosystem models simulate forest net ecosystem productivity (NEP) and evapotranspiration (ET) generally based on the explicit hypothesis of the influence of environmental factors on these fluxes (Ouyang et al., 2014). However, for both NEP and ET, there are discrepancies between bottom-up simulations from field observations and estimates from biosphere models (Piao et al., 2010; Zhang et al., 2014). These discrepancies are mainly attributed to a lack of mechanistic understanding of the environmental factors affecting carbon and water fluxes across multiple timescales (Ding et al., 2013; Jia et a., 2018), and the additional influence of abnormal environmental events (e.g., high- and cool-Ta). (Ouyang et al., 2014; Tian et al., 2020).

Variations in forest NEP (the balance between gross ecosystem productivity (GEP) and ecosystem respiration (RE)) and ET (the sum of plant transpiration and soil evaporation) are complex, because these flux components respond differently to environmental and biological factors, from daily to annual timescales (Baldocchi et al., 2018; Oishi et al., 2018). The GEP and plant transpiration represent carbon assimilation in ecosystem photosynthesis processes and plant water use, respectively,

* Corresponding author.
E-mail address: wenxf@igsnrr.ac.cn (X. Wen).

https://doi.org/10.1016/j.agrformet.2020.108310
Received 8 May 2020; Received in revised form 14 September 2020; Accepted 22 December 2020
Available online 21 January 2021

and these processes are mainly associated with variations in leaf stomatal conductance, plant phenology (e.g., plant growth stage) and canopy structure (e.g., enhanced vegetation index (EVI)) (Marcolla et al., 2011; van Gorsel et al., 2013). The RE includes autotrophic and heterotrophic respiration, and these processes are mainly associated with variations in plant root and soil microbe activities, litter fall input and carbon substrate availability (Aguilos et al., 2018; Baldocchi et al., 2018). Generally, environmental factors influence NEP and ET through their effect on biological processes (Baldocchi et al., 2008). At a daily timescale, NEP or ET are driven by diurnal cycles of solar energy factors (photosynthetically active radiation (PAR) or net radiation (Rn) and Ta) and vapor pressure deficit (VPD) through their effect on leaf stomatal, plant roots and soil microbe activities (Hong and Kim, 2011; Ouyang et al., 2014). From days to months timescales, synoptic weather patterns including high- and low-pressure systems may influence solar energy, VPD or soil water conditions, alter plant stomatal, phenology behaviors or canopy structure, with consequent variations in NEP or ET (Jia et al., 2018). Meanwhile, at an annual timescale, NEP and ET may respond to solar energy or soil water conditions, through their effect on plant phenology, growing season length or canopy structure (Baldocchi et al., 2018). In addition, the confounding effect of some environmental factors (e.g., PAR and Ta) that have similar cycles may obscure the specific effect of a factor on NEP or ET at multiple timescales (Ouyang et al., 2014; Jia et al., 2018). For example, although they were significantly correlated with NEP in an oak forest at both daily and annual timescales, Ouyang et al. (2014) indicated that PAR and Ta were the primary factors influencing NEP at daily and annual timescales, respectively, through their corresponding effects on leaf photosynthesis and leaf area. Investigating the specific effects of environmental factors on NEP and ET across multiple timescales is needed to determine the mechanisms by which environmental factors affect forest carbon and water fluxes.

High- or cool-Ta events may alter the variations in NEP and ET, and interact with the effects of environmental factors on NEP or ET (Granier et al., 2007; Tang et al., 2014). Generally, high-Ta may significantly decreased NEP (Jia et al., 2018) and ET (Ding et al., 2013), and enhanced the influence of VPD and soil water conditions on NEP or ET through its effect on leaf stomatal. However, the abnormal Ta event effect on NEP or ET may also be modulated by plant biological adjustments (e.g., absorbing deep soil water) (Bracho et al., 2008; Silvertown et al., 2015). For example, both scrub oak and pine flatwood forests can maintain ET during drought periods through absorbing deep soil water, and the resulting increased leaf area can compensate for decreased stomatal conductance (Bracho et al., 2008). Furthermore, previous studies indicated the impact of high- or cool-Ta events on NEP and ET may persist from daily to annual timescales (Baldocchi et al., 2018; Jia et al., 2018).Therefore, for a specific forest, there are still open discussions concerning the effects of high- and cool-Ta events on variations in NEP and ET, and on the influence of environmental factors on these fluxes across multiple timescales.

Wavelet analysis was used in this study to determine the temporal variability of carbon or water fluxes and the environmental factors affecting them, from daily to annual timescales, by decomposing these factors into the timescale domain signals. Previous studies demonstrated the suitability of wavelet analysis for non-stationary time series of environmental factors and carbon or water fluxes; the non-stationary pattern of these environmental factors and fluxes was mainly caused by precipitation pulses, heat waves or cold events (Vargas et al., 2011; van Gorsel et al., 2013; Koebsch et al., 2015). In this study, 11 years of half-hourly NEP and ET data were collected and analyzed using wavelet analysis for a subtropical coniferous plantation. The subtropical coniferous plantations of China represent more than 40% of the global subtropical forest area (Wen et al., 2010; Tang et al., 2016), and are sometimes exposed to surges of summer high-Ta and early spring cool-Ta (Zhang et al., 2011; Xu et al., 2017). We investigated (1) the variability of NEP and ET at multiple timescales and (2) the specific effect of environmental factors on these fluxes at multiple timescales, and the effect of summer high-Ta and early spring cool-Ta. We hypothesize that (1) both NEP and ET may exhibit time frequencies at daily and annual timescales that are affected by diurnal and annual variation of solar energy and (2) seasonal high- or cool-Ta effect on these fluxes may persist for timescales of up to an annual.

2. Material and methods

2.1. Study site

The study was conducted at Qianyanzhou station, located in Jiangxi Province in southeast China (26°44′52″N, 115°03′47″E), which is part of the ChinaFlux network. The average (mean ± SD) annual Ta and precipitation for 1985–2013 were 18.1 ± 0.7 °C and 1481.2 ± 254.9 mm, respectively. The daily Ta fluctuated from −5.8 to 39.8 °C, with the coefficient of variation was 72.2%. The lowest and highest annual precipitation amounts were 945 and 2410 mm, respectively. The soil is classified as a Typic Dystrudept based on United States soil taxonomy, with red mudstone and sandstone as the parent material (Tang et al., 2016). The total evergreen coniferous plantation tree density was 1338 stems ha^{-1} and was planted in 1985, dominated by slash pine (*Pinus elliottii* E., occupying 40.73%), Chinese fir (*Cunninghamia lanceolata* L., occupying 6.95%) and Masson pine (*Pinus massoniana* L., occupying 52.32%). The mean heights of three species were 14.31 ± 2.53, 11.8 ± 1.39 and 11.25 ± 2.07 m, respectively. *Loropetalum chinense* and *Arundinella setosa* were dominant shrub and herbaceous species in the studied plantation.

2.2. Eddy covariance and environmental factor observation

The NEP and ET were observed through an eddy covariance system mounted at 39.6 m above ground on a tower since 2003. The system consists of a 3-D sonic anemometer (CSAT3, Campbell Scientific Inc., Logan, UT, USA), and an open-path CO_2/ H_2O analyzer (Li-7500, Li-Cor Inc., Lincoln, NE, USA). A CR3000 datalogger (Campbell Scientific Inc.) was used to calculate and store the 10-Hz raw data and 30-min average values.

Environmental factors such as PAR (LI-190SB, Li-Cor Inc.), Ta, and relative humidity (HMP45C, Campbell Scientific Inc.) were measured at 23.6 m above ground. Soil heat flux (5 cm depth below ground) and soil water content (SW) (20 and 50 cm depth below ground, SW_20 cm and SW_50 cm) were measured with two plates (HFT-3, Campbell Scientific Inc.) and TDR probes (CS615-L, Campbell Scientific Inc.), respectively. Soil temperatures (20 cm depth below ground) were measured with thermocouples (105T and 107-L, Campbell Scientific Inc.). Precipitation amount was monitored with a rain gage (52,203, RM Young Inc., Traverse City, MI, USA). A CR1000 datalogger (Campbell Scientific Inc.) was used to measure and store all 30-min average environmental factors. More details are provided in Wen et al. (2010) and Tang et al. (2016).

2.3. Flux data processing

First, planar fit rotation and the Webb–Pearman–Leuning method were used to remove the instrument tilt of the airflow (Wilczak et al., 2001) and air density fluctuation (Webb et al., 1980) for 30-min average carbon and water fluxes, respectively. Missing or abnormal carbon or water fluxes data were excluded during flux data processing. These missing or abnormal data were generally caused by instrument malfunction, and data quality control such as sonic anemometer error and open-path analyzer interference generated by rainfall (Wen et al., 2010), as well as CO_2 and water vapor density outside reasonable bounds and exceeding four times the standard deviation at 4-h intervals (Tang et al., 2016). Carbon and water fluxes at nighttime (solar elevation angle < 0) were also excluded when friction velocity < 0.19 m s^{-1}, calculated using the method of Reichstein et al. (2005), to avoide possible

underestimation of these fluxes under stable conditions at night. Annual average data gaps accounted for 31.72 ± 9.5 and 29.98 ± 9.32% of the total data for carbon and water fluxes, respectively, with approximately 70% of data gaps for these fluxes occurring during nighttime.

Then, data gaps of NEP and ET smaller than 2 h were filled by linear interpolation. Carbon flux gaps longer than 2 h were filled separately for daytime and nighttime. Nighttime carbon flux (RE at nighttime) gaps longer than 2 h were filled using SW and soil temperature as suggested in Reichstein et al. (2005), with the equation parameters estimated by fitting the equation to nighttime available carbon flux and environmental factor data at 3-month intervals. Subsequently, assuming the consistency of environmental factors' sensitivity for daytime and nighttime RE (Wen et al., 2010), the obtained equation parameters were then used to estimate the daytime RE using daytime SW and soil temperature. The daytime CO_2 flux (NEP) gaps longer than 2 h were filled using the Michaelis–Menten equation, with the parameters obtained by fitting the equation to daytime available NEP and corresponding environmental factors at 10-day intervals (Falge et al., 2001). The GEP was calculated as the sum of NEP and daytime and nighttime RE. Finally, the look-up table method was used to fill ET gaps longer than 2 h (Falge et al., 2001).

The flux footprint varied seasonally associated with the prevailing wind direction, which was northwest in winter and southeast in summer (Zhang and Wen, 2015). Meanwhile, the 90% annual flux footprint areas ranging from 11.01 (2012) to 12.44 km^2 (2003), with the average area was 11.72 ± 0.95 km^2, calculated using the method in Zhang and Wen (2015). In addition, the energy balance ratio (*EBR*) was used to assess the eddy covariance performance (Wilson et al., 2002) in Eq. (1):

$$EBR = (LE + H)/(Rn - G - S) \quad (1)$$

where *LE* and *H* are the latent and sensible heat fluxes, respectively, and *Rn, G* and *S* are the net radiation, soil and storage heat fluxes, respectively; *S* is the sum of latent and sensible storage heat fluxes, and calculated using the method of Moore et al. (1986). The units of all variables in the right-hand side of this equation are W m^{-2}. The average *EBR* (0.72 ± 0.06) was slightly smaller than the value at FLUXNET sites (0.79), and within the range of 0.53–0.99 (Wilson et al., 2002).

2.4. Data analysis

2.4.1. Summer high-Ta and early spring cool-Ta periods

The high-Ta period in Southern China was defined as the days with daily maximum Ta higher than 35 °C and lasting more than 7 days (Zhang et al., 2005). In the present study, most of the high-Ta period occurred in July and August in 2003, 2007 and 2010 (Table 1). The high-Ta corresponding period in all years except 2003, 2007 and 2010 was determined to be 10 July to 13 August for subsequent wavelet and statistical analyses. Furthermore, July to August in 2003, 2007 and 2010 were considered as drought periods according to the monthly Budyko's aridity index (the ratio of precipitation amount to potential ET) in our previous study (Tang et al., 2016). The significantly lower SW_20 cm and SW_50 cm ($P < 0.05$) was also observed during the high-Ta period, compared with the value of the corresponding period in all years except 2003, 2007 and 2010. The detailed statistical analysis method and results are given in Section 2.5 and 3.1, respectively.

The cool-Ta period in the studied region was defined as the days with daily average Ta lower than 5 °C and lasting more than 7 days (Zhang et al., 2011; Xu et al., 2017). In the present study, the cool-Ta period mostly occurred in January and February in 2005, 2008 and 2011 (Table 1). Similarly, the cool-Ta corresponding period in all years except 2005, 2008 and 2011 was determined to be 4 January to 13 February for subsequent wavelet and statistical analyses.

2.4.2. Wavelet analysis

Wavelet analysis can be used to quantify the variance of a specific time series and correlations between different time series across multiple timescale frequencies (Grinsted et al., 2004; Hong and Kim, 2011; Jia et al., 2018).

The wavelet power spectrum (S_n), calculated by continuous wavelet transform (CWT), can be used to describe the variability for specific time series (x_n) in Eq. (2):

$$S_n(s) = \left|W_n^x(s)\right|^2 = \left|\sqrt{\delta t/s}\sum_{n'=0}^{N-1} x_n \psi^*(((n' - n)\delta t)/s)\right|^2 \quad (2)$$

where W_n^x is the CWT coefficient of time series x_n; s is the wavelet scale; δ_t is sampling interval, which is 30-min in this study; ψ^* is the complex conjugate; n is the local time index from 1 to N; N is the number of points of x_n; and n' is the time variable.

The effect of an environmental factor (x) on NEP or ET (y) can be calculated through the wavelet coherence (WTC) spectrum ($R^2_n(y, x)$) in Eq. (3):

$$R^2_n(y,x) = \left|S\left(s^{-1}W_n^{xy}(s)\right)\right|^2 \Big/ \left(\left|S\left(s^{-1}W_n^{x}(s)\right)\right|^2 \left|S\left(s^{-1}W_n^{y}(s)\right)\right|^2\right) \quad (3)$$

where S is the smoothing in time and scale, and $W_n^{xy}(s)$ is the cross spectrum between x and y; $W_n^x(s)$ and $W_n^y(s)$ are the CWT of x and y, respectively.

The partial wavelet coherence (PWC) was used to determine the effect of x_1 on y after removing the influence of x_2 through the PWC spectrum ($RP^2_n(y, x_1, x_2)$) in Eq. (4):

$$RP^2_n(y,x_1,x_2) = \left(R_n(y,x_1) - R_n(y,x_2)R_n(y,x_1)^*\right)^2 \Big/ \left((1 - R_n(y,x_2))^2(1 - R_n(x_2,x_1))^2\right) \quad (4)$$

where $R_n(y, x_1)$, $R_n(y, x_2)$ and $R_n(x_2, x_1)$ are the WTC spectra between y and x_1, y and x_2, and x_2 and x_1, respectively; $R_n(y, x_1)^*$ is the complex conjugation of the WTC spectrum between y and x_1. For example, the specific effect of PAR on NEP was detected after removing the influence of Ta, VPD, SW_20 cm and SW_50 cm, with the PWC spectrum calculated as RP^2_n(*NEP, PAR, Ta*), RP^2_n(*NEP, PAR, VPD*), RP^2_n(*NEP, PAR, SW_20 cm*) and RP^2_n(*NEP, PAR, SW_50* cm), respectively.

Table 1
Time range and averaged air temperature (Ta, °C) of high-Ta and cool-Ta periods.

Period	Time range	Average Ta	Time range	Average Ta	Time range	Average Ta
High-Ta	2003 10 July-4 August	37.2 ± 1.7	2007 18 July-3 August	36.5 ± 0.9	2010 30 July-13 August	35.8 ± 0.7
Cool-Ta	2005 6 January-3 February	3.3 ± 1.4	2008 13 January-13 February	1.0 ± 1.3	2011 4 January-2 February	2.2 ± 1.3

The phase angle spectrum (A_n) was used to determine the phases and amplitudes between x and y in WTC analysis:

$$A_n(s) = \tan^{-1}\left(\mathrm{Im}\left(W_n^{xy}(s)\right) / \mathrm{Re}\left(W_n^{xy}(s)\right)\right) \quad (5)$$

where $\mathrm{Im}(W_n^{xy}(s))$ and $Re(W_n^{xy}(s))$ are the imaginary and real parts of the cross spectrum between x and y, respectively. The A_n (lag time) can be described and visualized through arrows in WTC analysis. Arrows pointing right indicate no phase between x and y; arrows pointing left indicate x lagging y by 180°; arrows pointing down indicate x leading y by 90°; and arrows pointing up indicate x lagging y by 90°

In the present study, the global wavelet spectrum during CWT analysis was used to identify the timescales that exhibited the peak variability for NEP, ET and environmental factors. This method was also used to detect the gap filling effect on the result of CWT analysis for NEP and ET, by comparing results between gap-filled and non-gap-filled fluxes. These data gaps for both NEP and ET were filled with zero during CWT analysis. Then, WTC analysis was used to quantify the local correlation between gap-filled NEP (or ET) and environmental factors (PAR (or Rn), Ta, VPD, SW_20 cm and SW_50 cm) at different timescales through averaged wavelet coherency and the phase angle spectrum. Finally, PWC analysis was used to detect partial correlations between gap-filled NEP (or ET) and environmental factors at different timescales based on averaged wavelet coherency and the phase angle spectrum. The significance of the wavelet spectrum for CWT, WTC and PWC analysis was determined at 0.05 level by the Monte Carlo method (Ouyang et al., 2014).

The dominant environmental factor affecting NEP or ET was selected by the response time calculated through the phase angle spectrum, as suggested in Koebsch et al. (2015) and Jia et al. (2018). First, the proportions of significant WTC and PWC data were calculated based on criteria of 0.05 significance level and the cone of influence (COI). Then, the phase angle (lag time) at the specific timescale was calculated through WTC based on two criteria: (1) the averaged wavelet coherency spectrum higher than 0.5 and (2) the significance wavelet spectrum data occupied more than 30% total data. The smallest lag time was used to determine the dominant factor synchrony with NEP or ET among the environmental factors. In addition to WTC and PWC analysis, the General Additive Modeling (*GAM*) calculated using the "mgcv" package in R software (version 4.0.2, R Core Team, 2020) was used to identify the dominant environmental factor affecting NEP and ET at daily, 30-day and annual timescales. Firstly, the *step* method in R software was used to determine the significance influence of each environmental factor, including PAR (Rn), Ta, VPD, SW_20 cm and SW_50 cm, on NEP (ET) at each timescale. Then, environmental factors that remained in the final equation generated using the *step* method were used in the GAM model, and the environmental factor with the largest deviance explanation (%) was considered to be the dominant effect on NEP or ET at each timescale.

Furthermore, the influence of summer high-Ta on the time lag between environmental factors and NEP (or ET) was determined by comparing the averaged WTC results for 2003, 2007 and 2010, and the average value for the other years from 10 July to 13 August. The influence of early spring cool-Ta on the time lag between environmental factors on NEP (or ET) was determined by comparing the averaged WTC results for 2005, 2008 and 2011, and the average value for the other years from 4 January to 13 February. All wavelet analyses were conducted using Matlab R2014, and the codes were described by Grinsted et al. (2004).

2.5. Statistical analysis

One-way ANOVA was used to determine the significant effects of high- and cool-Ta on daily PAR, Rn, VPD, SW_20 cm, SW_50 cm, NEP and ET. First, significant differences for daily averages of each factor between high-Ta period of 2003, 2007 and 2010, and the daily averaged value of the other years from 10 July to 20 August were detected. Then, the significant differences for daily averages of each factor between cool-Ta period of 2005, 2008 and 2011, and the daily averaged value of the other years from 4 January to 13 February were detected. All statistical analyses mentioned above were conducted using SPSS 22.0 software, after data normality was checked and homogeneity of variance was assessed.

3. Results

3.1. Variabilities of environmental factors, NEP and ET

The PAR, Rn, Ta and VPD exhibited similar seasonal patterns with single summer peaks and lower values during winter and spring (Fig. 1). The seasonal SW_20 cm and SW_50 cm variation followed that of precipitation. The lower SW in summer in 2003, 2007 and 2010 coincided with lower amounts of precipitation and higher Ta and VPD. The daily averaged PAR (36.95 ± 7.84 mmol m^{-2}), Ta (31.6 ± 1.6 °C) and VPD (1.72 ± 0.44 kPa) during high-Ta period in 2003, 2007 and 2010 were significantly higher ($P < 0.05$) and 1.13, 1.1 and 1.65 times the average values during the corresponding period in the other years, respectively. Meanwhile, the daily averaged SW_20 cm (0.25 ± 0.01 m^3 m^{-3}) and SW_50 cm (0.31 ± 0.01 m^3 m^{-3}) were significantly lower ($P < 0.05$) and only accounted for 78.39 and 82.55% of the average values during the corresponding period in the other years. The lower-Ta during spring in 2005, 2008 and 2011 coincided with lower PAR and Rn. The daily averaged PAR (6.29 ± 5.58 mmol m^{-2}), Rn (1.91 ± 1.7 W m^{-2}), Ta (2.2 ± 1.8 °C) and VPD (0.08 ± 0.06 kPa) during the cool-Ta period in 2005, 2008 and 2011 were significantly lower ($P < 0.05$) and accounted for only 66.58, 66.84, 31.62 and 44.48% of the average values during the corresponding period in the other years. However, there was no significant variation in SW_20 cm and SW_50 cm between the cool-Ta period in 2005, 2008 and 2011, and the corresponding period in the other years.

The NEP and ET exhibited single peak patterns with higher values occurring during summer, and lower value during winter and spring. The daily averaged NEP (0.59 ± 0.53 g C m^{-2}) and ET (3.46 ± 1.13 mm) during high-Ta period in 2003, 2007 and 2010 were significantly lower ($P < 0.05$), and accounted for 31.42 and 86.12%, respectively, of the average values during the corresponding period in the other years (Fig. S1). The daily averaged NEP (0.27 ± 0.51 g C m^{-2}), but not ET (0.78 ± 0.41 mm), during the cool-Ta period in 2005, 2008 and 2011 was significantly lower, and accounted for 67.8% ($P < 0.05$) and 89.6% ($P = 0.06$) of the average values during the corresponding period in the other years (Fig. S2).

There were almost no differences in wavelet power spectra between non gap-filled and gap-filled NEP or ET (Fig. 2). Therefore, the global wavelet power spectra of gap-filled NEP and ET were analyzed. In general, the global wavelet power spectra of PAR, Rn, VPD, NEP and ET exhibited significant strong peaks at both daily and annual timescales, with Ta exhibiting strong but non-significant peaks at daily timescale (Fig. 3 and S3). There were also significant spectrum peaks longer than 180-days for NEP, and longer than 16-days for ET (Fig. 3). The SW_20 cm and SW_50 cm exhibited significant peaks only for timescales longer than 8 days. Variations were also observed from days to months timescales for these environmental factors (Fig. 3 and S3). Furthermore, NEP but not ET exhibited strong peaks at longer than 500-day timescales.

3.2. Correlations and time lags between NEP, ET and environmental factors

3.2.1. Daily timescale

The PAR exhibited the strongest synchrony with NEP at the daily timescale, followed by Ta and VPD, based on time lag (Table 1, Fig. 4). At this timescale, NEP preceded PAR by 1.12 ± 0.24 h, and preceded Ta and VPD by more than 4 h. A significant effect of PAR on NEP was also

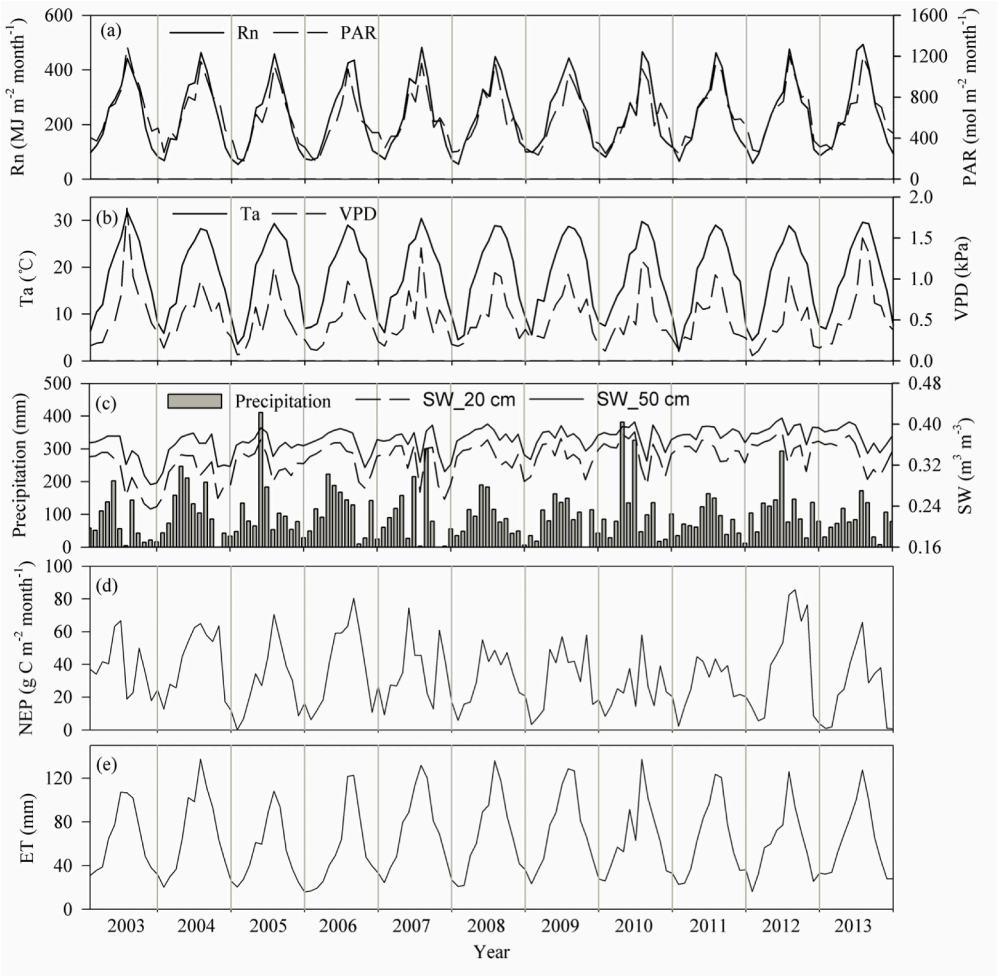

Fig. 1. Monthly variations of (a) net radiation (Rn) and photosynthetically active radiation (PAR), (b) air temperature (Ta) and vapor pressure deficit (VPD), (c) precipitation amount and soil water content at 20 and 50 cm depth (SW_20 cm and SW_50 cm), (d) ecosystem productivity (NEP) and (e) evapotranspiration (ET) during 2003–2013.

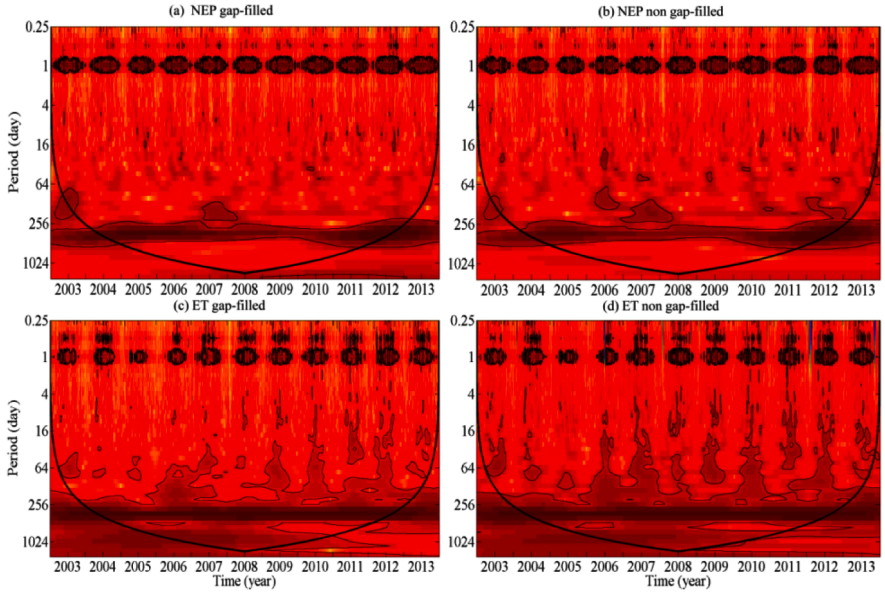

Fig. 2. Wavelet power spectrum for (a) gap-filled NEP, (b) non gap-filled NEP, (c) gap-filled ET and (d) non gap-filled ET. Both $P < 0.05$ level and the COI are shown as thick lines. The blue and red colors represent low and high wavelet power values, respectively. (For interpretation of the references to colour in this figure legend, the reader is referred to the web version of this article.)

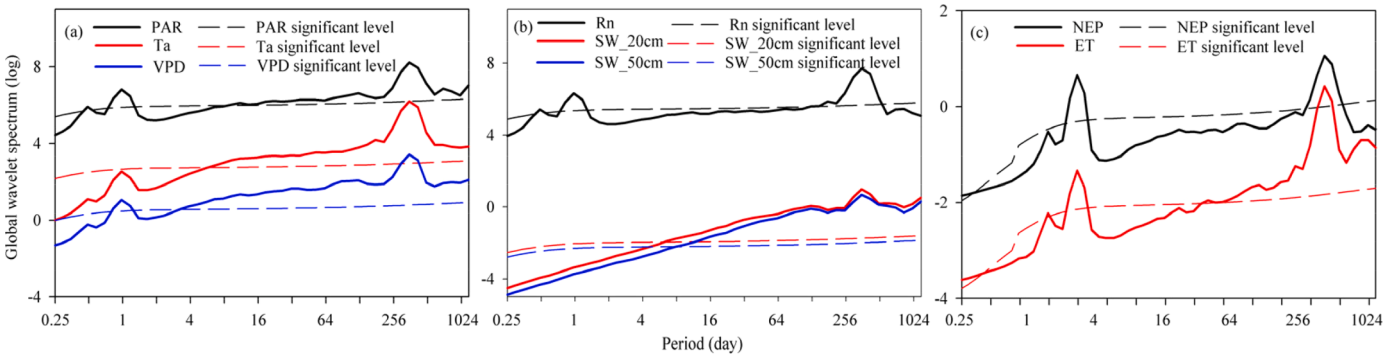

Fig. 3. Global wavelet spectrum for (a) PAR, Ta, VPD, (b) Rn, SW_20 cm and SW_50 cm and (c) NEP and ET. The wavelet spectra were $\log_{10}$ transformed.

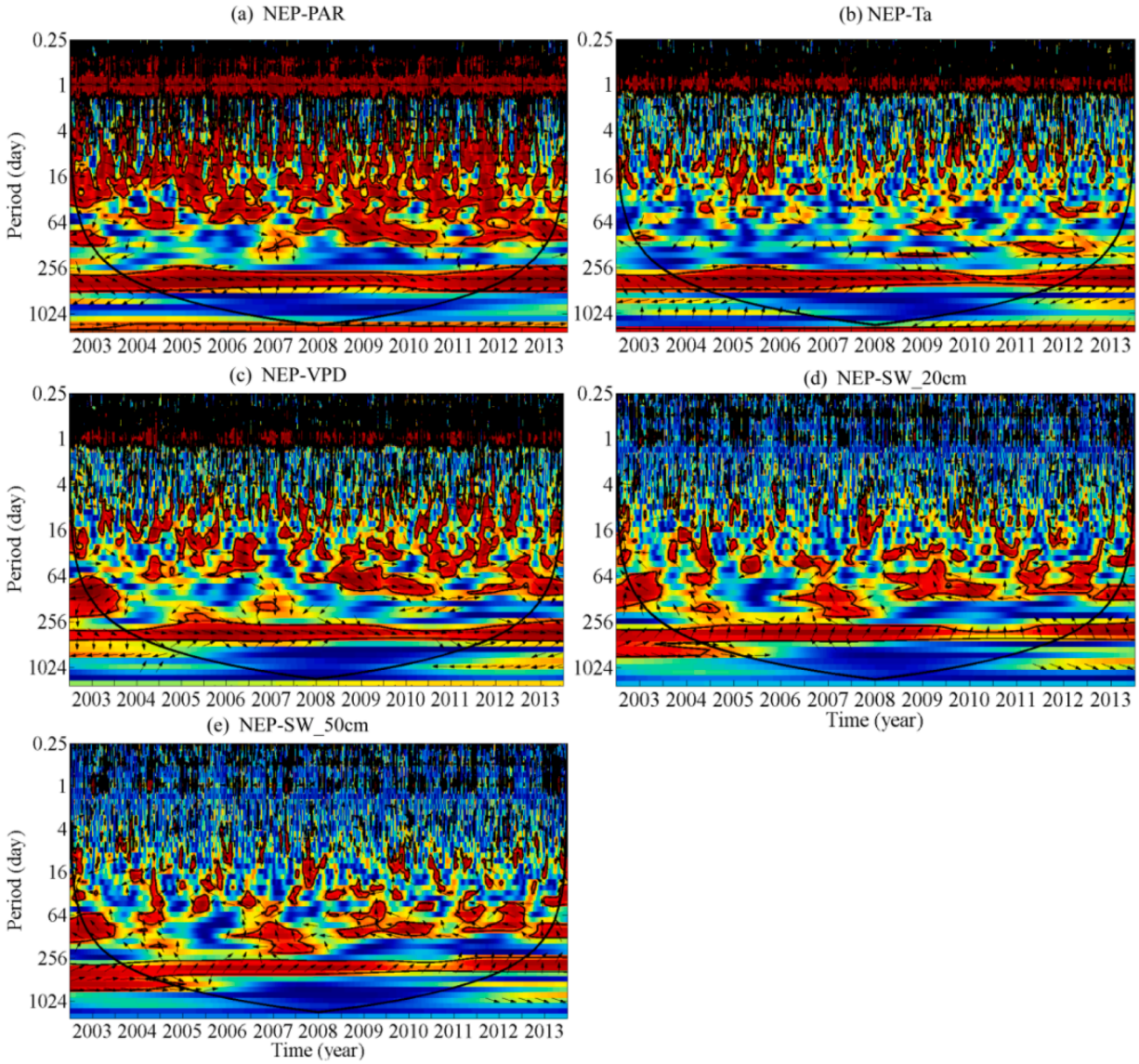

Fig. 4. Wavelet coherence between NEP and (a) PAR, (b) Ta, (c) VPD, (d) SW_20 cm and (e) SW_50 cm. Both $P < 0.05$ level and the COI are shown as thick lines. The blue and red colors represent low and high wavelet power values, respectively. The arrows indicate the phase between NEP and environmental factors. (For interpretation of the references to colour in this figure legend, the reader is referred to the web version of this article.)

observed after removing the effect of other environmental factors (except Ta) at a daily timescale, based on the PWC results (Table S1, Fig. 5). However, at a daily timescale, there was no significant effect of Ta, VPD, SW_20 cm and SW_50 cm on NEP after removing the effect of PAR (Table S1).

The Rn exhibited the strongest synchrony with ET at a daily timescale, followed by VPD and Ta (Table 2, Fig. 6). The Rn preceded ET by 1.16 ± 0.8 h, and preceded VPD and Ta by more than 3 h. Based on the

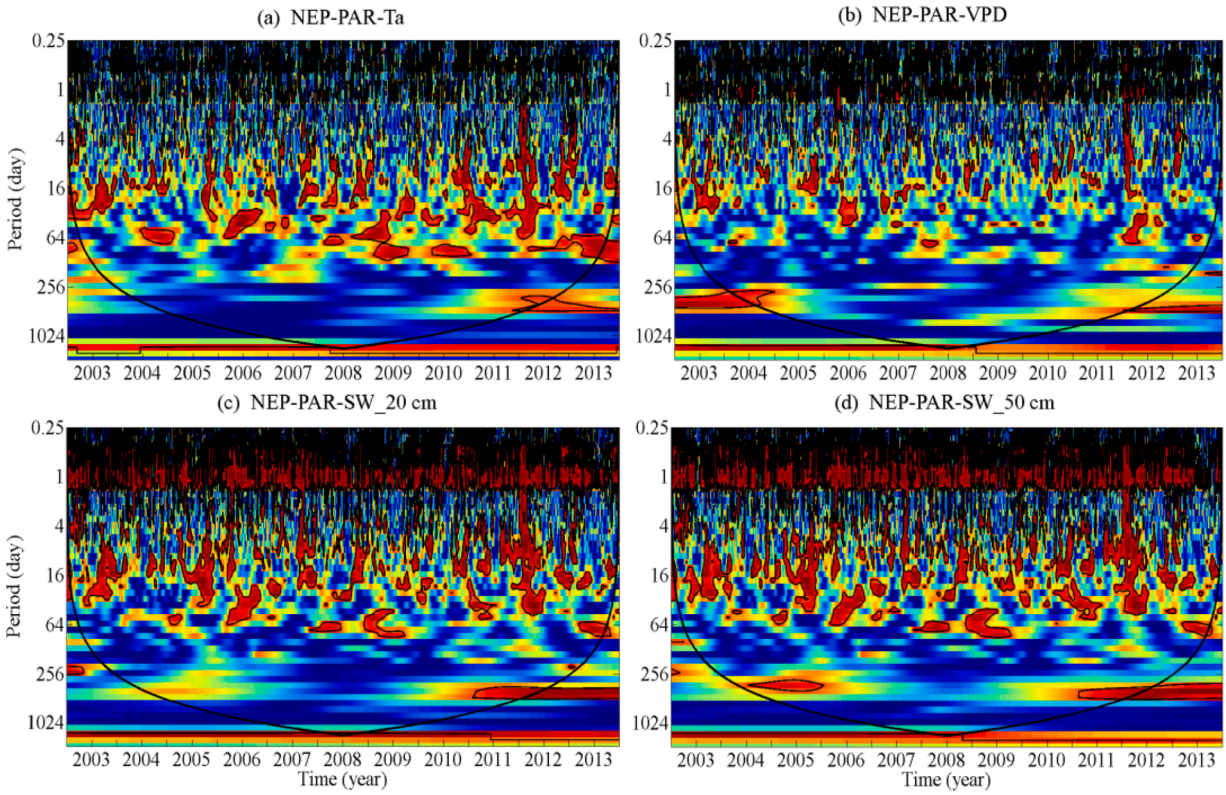

Fig. 5. Partial wavelet coherence between NEP and PAR among multiple timescales after removing the effect of (a) Ta, (b) VPD, (c) SW_20 cm and (d) SW_50 cm. Both $P < 0.05$ level and the COI are shown as thick lines. The blue and red colors represent low and high wavelet power values, respectively. (For interpretation of the references to colour in this figure legend, the reader is referred to the web version of this article.)

Table 2
Percentage of time with significant correlations, average wavelet coherency and time lag (mean ± SD) between NEP and PAR, Ta, VPD, SW_20 cm and SW_50 cm among multiple timescales.

Period	PAR		Ta		VPD		SW_20 cm		SW_50 cm	
	%	Time lag	%	Time lag	%	Time lag	%	Time lag	%	Time lag
daily	99.87	1.12 ± 0.24	96.29	4.22 ± 1.59	89.68	4.82 ± 1.69	21.51	–	22.54	–
8day	59.07	0.57 ± 1.01	31.95	2.81 ± 1.66	34.4	1.58 ± 1.2	19.86	–	18.26	–
30day	50.65	1.72 ± 3.5	6.47	–	34.18	3.62 ± 5.1	28.46	–	19.04	–
60day	37.86	4.32 ± 8.53	0.3	–	29.36	–	31.2	−36.45 ± 15.97	28.98	–
120day	15.74	–	7.37	–	6.13	–	25.72	–	27.16	–
360day	75.97	30.94 ± 18.77	75.97	23.16 ± 17.01	75.97	27.38 ± 16.24	75.97	−151.26 ± 28.93	75.97	−102.46 ± 20.49

According to time lag, hours were used for daily timescale and days for the other timescales. The "-" of time lag indicates the percentage of time with significant correlations less than 30% and wavelet coherency spectrum smaller than 0.5 at a specific timescale.

PWC result, Rn still significantly affected ET at a daily timescale, after removing the effect of other environmental factors (except Ta) (Table S1, Fig. 7). However, there was no significant effect of Ta, VPD, SW_20 cm, SW_50 cm on ET at a daily timescale, when removing the effect of Rn (Table S1). In addition, consistent with the wavelet analysis, the GAM result showed that PAR and Rn were the dominant factors influencing NEP (Table S2) and ET (Table S3), respectively, at a daily timescale.

3.2.2. *Days to months timescales*

The PAR exhibited the strongest synchrony with NEP from 4 to 0-days timescales; meanwhile, NEP was also influenced by VPD and SW_20 cm at a longer than 30-day timescale (Table 1, Fig. 4). The NEP preceded PAR and VPD, but lagged SW_20 cm at these timescales. Based on the PWC result, PAR exhibited no continuous significant synchrony with NEP after removing the effects of Ta, VPD, SW_20 cm and SW_50 cm for timescales of days to months (Table S1, Fig. 5). Additionally, there was no significant effect of Ta, VPD, SW_20 cm and SW_50 cm on NEP after removing the effect of PAR from these timescales (Table S1).

The Rn exhibited the strongest synchrony with ET at 8-, 30- and 120-day timescales, and VPD also significantly affected ET at 8- and 90-day timescales (Table 2). The ET preceded Rn and VPD at these timescales, however, there was no significant effect of SW_20 cm and SW_50 cm on ET at these timescales. In addition, Rn only exhibited synchrony with ET at 120-day timescale after removing the effect of Ta, and no continuous effect was observed between Rn and ET after removing the effect of other environmental factors for days to months timescales (Table S1, Fig. 7). However, there were no significant effects of Ta, VPD, SW_20 cm and SW_50 cm on ET after removing the effect of Rn at these timescales (Table S1). Furthermore, consistent with the wavelet analysis, the GAM result showed that PAR and Rn were the dominant factors influencing NEP and ET, respectively, at the 30-day timescale (Table S4).

3.2.3. *Annual timescale*

At an annual timescale, Ta exhibited the strongest synchrony with NEP; and NEP preceded Ta, VPD and PAR by 23.16 ± 17.01, 27.38 ±

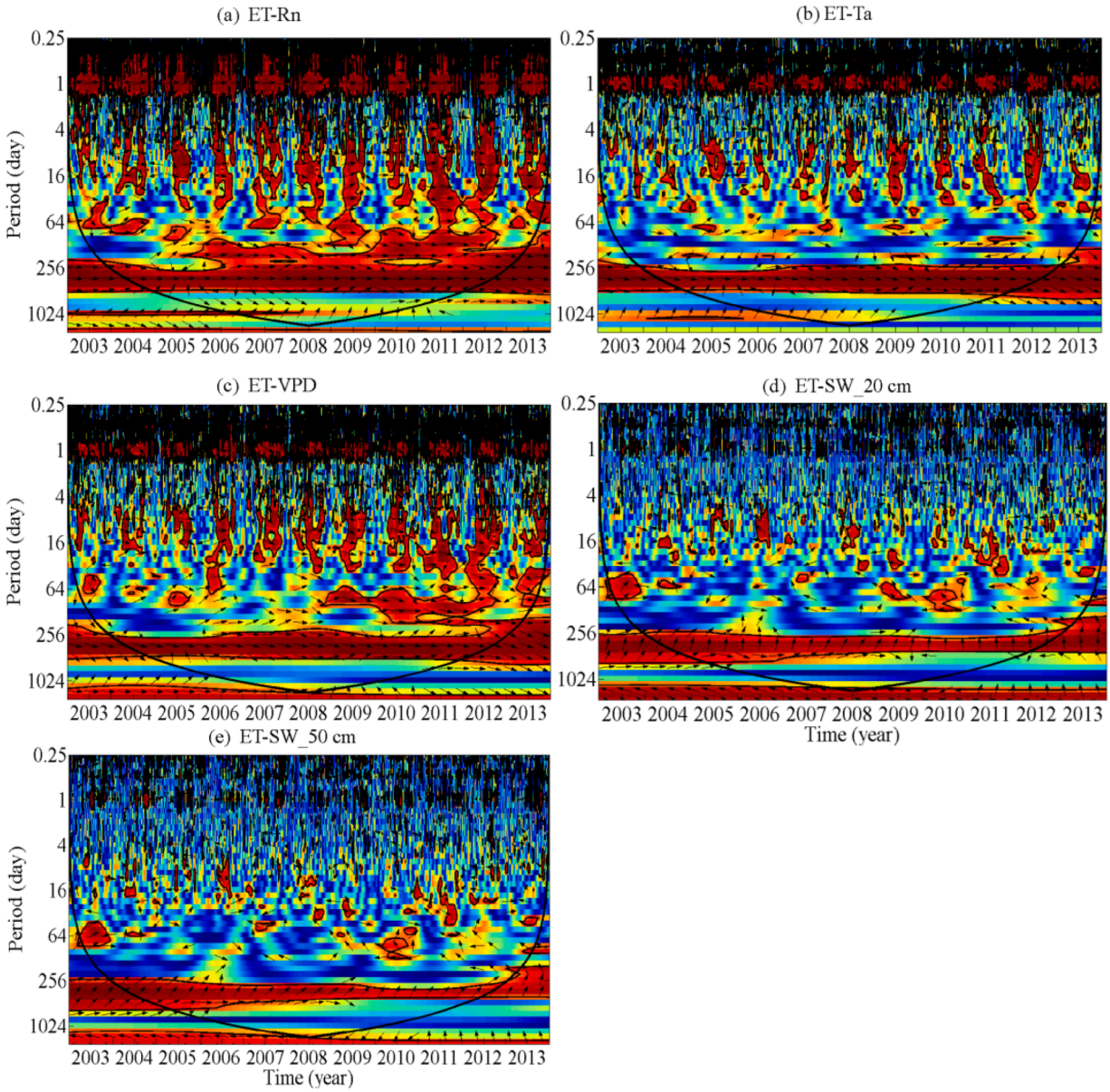

Fig. 6. Wavelet coherence between ET and (a) Rn, (b) Ta, (c) VPD, (d) SW_20 cm and (e) SW_50 cm. Both $P < 0.05$ level and the COI are exhibited as thick lines. The blue and red colors represent low and high wavelet power values, respectively. The arrows indicate the phase between ET and environmental factors. (For interpretation of the references to colour in this figure legend, the reader is referred to the web version of this article.)

16.24 and 30.94 ± 18.77 days, respectively (Table 1, Fig. 4). Meanwhile, the NEP lagged SW_20 cm and SW_50 cm by 151.26 ± 28.93 and 102.46 ± 20.49 days, respectively, at an annual timescale (Table 1). There was no significant effect of PAR on NEP after removing the effect of other environmental factors (Table S1, Fig. 5). In addition, at this timescale, there was no significant effect of Ta, VPD, SW_20 cm and SW_50 cm on NEP after removing the effect of PAR (Table S1).

At an annual timescale, Rn exhibited the strongest synchrony with ET; and ET preceded Rn, Ta and VPD by 5.73 ± 4.39, 18.04 ± 3.7 and 22.24 ± 6.15 days, respectively (Table 1, Fig. 6). Similar to NEP at this timescale, ET lagged SW_20 cm and SW_50 cm by 159.19 ± 19.27 and 108.76 ± 15.3 days, respectively (Table 2, Fig. 6). The Rn also showed significant synchrony with ET after removing the effect of other environmental factors (except Ta) (Table S1, Fig. 7); there was no significant effect of other environmental factors on ET following removal of the effect of Rn (Table S1). Furthermore, inconsistent with the wavelet analysis, the GAM result showed that no environmental factor was dominant in the annual variations of NEP and ET (Table S5).

3.3. *Effect of summer high-Ta on NEP and ET*

Summer high-Ta enhanced the influence of SW_20 cm and SW_50 cm on NEP, and weakened the influence of VPD on NEP, at a daily timescale (Table S6). The summer high-Ta generally weakened the effect of PAR, Ta and VPD on NEP shorter than 30-day timescales, but enhanced the effect of PAR and VPD at 120-day timescale especially in 2003. The summer high-Ta enhanced the effect of SW_20 cm and SW_50 cm on NEP at 120-day timescale, even after removing the effect of PAR and Ta (Table S6, Fig. S4). Summer high-Ta also shortened the time lag of VPD and SW on NEP at an annual timescale (Table S6).

Summer high-Ta enhanced the effect of SW_20 cm and SW_50 cm on ET at a daily timescale (Table S7). Summer high-Ta enhanced the effect of SW_20 cm and SW_50 cm on ET at 60- and 120-day timescales especially in 2003, even after removing the effect of Rn and Ta (Fig. S5). Similar to NEP, high-Ta also shortened the time lag of VPD and SW on ET at an annual timescale.

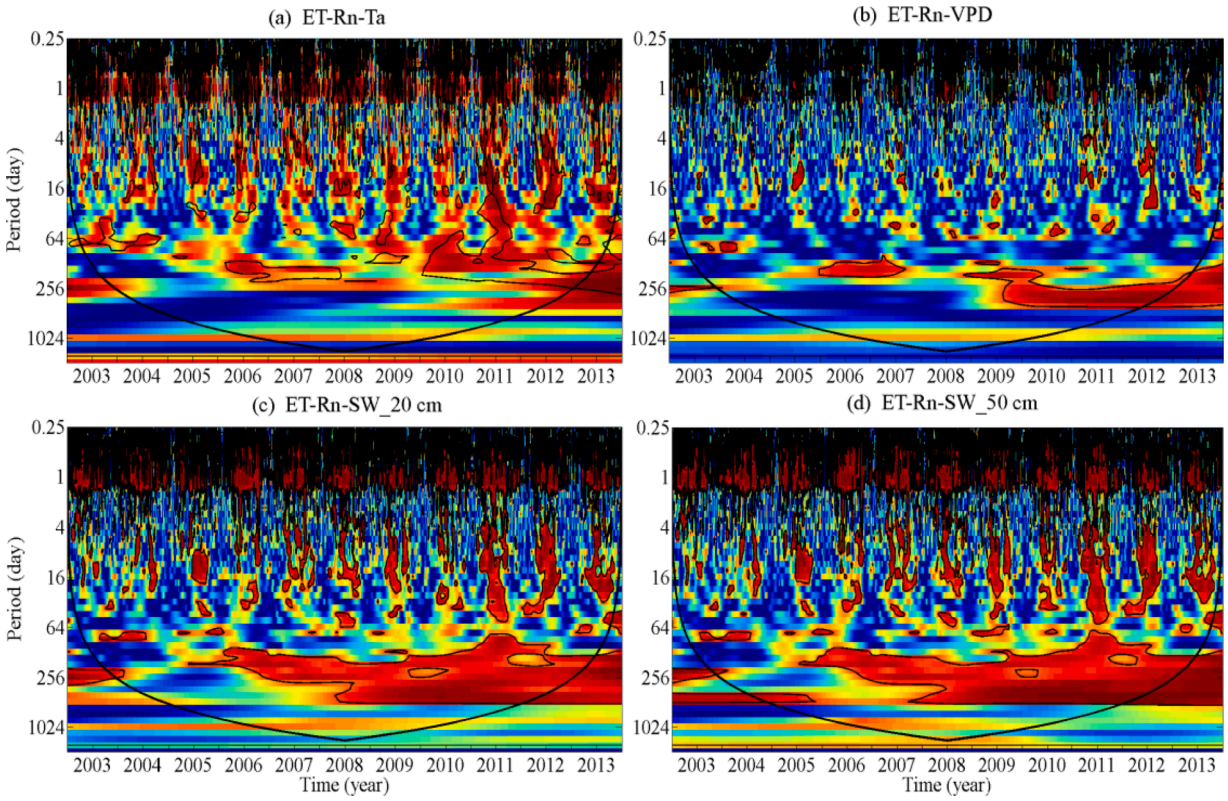

Fig. 7. Partial wavelet coherence between ET and Rn among multiple timescales after removing the effect of (a) Ta, (b) VPD, (c) SW_20 cm and (d) SW_50 cm. Both $P < 0.05$ level and the COI are exhibited as thick lines. The blue and red colors represent low and high wavelet power values, respectively. (For interpretation of the references to colour in this figure legend, the reader is referred to the web version of this article.)

3.4. Effect of early spring cool-Ta on NEP and ET

Early spring cool-Ta shortened the time lag between PAR and NEP at daily, 30- and 60-day timescales, and weakened the effect of SW_20 cm on NEP at 60-day timescale (Table S8). However, early spring cool-Ta enhanced the effect of VPD on NEP at 30- and 120-day timescales, especially in 2008. The early spring cool-Ta shortened the time lag between VPD, SW_20 cm, SW_50 cm and NEP at an annual timescale.

Early spring cool-Ta shortened the time lag between Ta, VPD and ET at a daily timescale, and weakened the effect of Rn and VPD on ET for timescales shorter than 30-day (Table S9). In contrast to the case of NEP, cool-Ta did not affect the time lag between these environmental factors on ET at an annual timescale.

4. Discussion

4.1. Solar energy dominates and soil water modulates the variations of NEP and ET

4.1.1. Solar energy dominates the variations of NEP and ET at a daily timescale

The significant peak of wavelet global power spectra for NEP and ET at a daily timescale indicated the strong diurnal fluctuations of these fluxes, with peak value occurring in daytime and relative constant or close to zero value during nighttime. The strong diurnal fluctuation of these fluxes is generally associated with diurnal fluctuations of the solar energy factors through their effect on forest photosynthesis and transpiration (Baldocchi et al., 2008; Ding et al., 2013). Generally, GEP represents the canopy photosynthesis and is a function of PAR (van Gorsel et al., 2013; Baldocchi et al., 2018), and RE is the carbon release and is influenced by temperature, SW and carbon substrate supply through photosynthesis processes (Oishi et al., 2018). There are two stands of evidence suggesting that the NEP was associated with the forest photosynthesis process at a daily timescale in the studied plantation: (1) GEP rather than RE exhibited a similar wavelet global power spectrum to that of NEP; (2) GEP exhibited a high coherence of its spectrum with that of NEP, and there was no appreciable time lag between these fluxes (Fig. S6). In addition, in the studied plantation, Niu et al. (2019) and Mi et al. (2009) indicated that more than 70% of the ET was occupied by plant transpiration based on the Priestly–Taylor Jet Propulsion Laboratory model and Ecological Assimilation of Land and Climate Observations model, respectively. Therefore, plant transpiration was mainly considered to interpret the variation of ET in the studied coniferous plantation. Consistent to the first hypothesis, the shortest time lag (1.12 ± 0.24 h) between NEP and PAR among environmental factors in the present study indicated the fastest response of NEP to variation in PAR, and suggested that PAR was the primary environment factor influencing NEP at a daily timescale (Table 2, Fig. 4). Meanwhile, the Rn was the main factor influencing ET in the studied plantation, with the shortest time lag (1.16 ± 0.8 h) at a daily timescale (Table 3, Fig. 6), associated with variations in plant transpiration that were affected by stomatal conductance (van Gorsel et al., 2013; Xu et al., 2020). Our previous studies also proved that canopy conductance, calculated through the Penman–Monteith equation (Kelliher et al., 1995), significantly influenced the daily ET (Tang et al., 2014).

Short time lag was observed between PAR and NEP in a temperate forest (Koebsch et al., 2015) and a wetland ecosystem (Ouyang et al., 2014) at a daily timescale; Aguilos et al. (2018) attributed this in-phase behavior to sufficient water supply conditions. In addition, previous studies attributed the peak values of NEP or ET occurring before the peak values of VPD, which generally occurred at noon, to the stomatal regulation in response to possible water-limited conditions (Ouyang et al., 2014; Oishi et al., 2018). In the present studied plantation, both NEP and ET exhibited peak values 4.82 ± 1.69 and 3.45 ± 2.1 h,

Table 3
Percentage of time with significant correlations, average wavelet coherency and time lag (mean ± SD) between ET and Rn, Ta, VPD, SW_20 cm and SW_50 cm among multiple timescales.

Period	Rn		Ta		VPD		SW_20cm		SW_50cm	
	%	Time lag	%	Time lag	%	Time lag	%	Time lag	%	Time lag
daily	89.86	−1.16 ± 0.8	85.04	3.54 ± 2.08	87.44	3.45 ± 2.1	22.11	–	20.15	–
8day	41.38	0.09±0.64	24.53	–	38.98	0.68 ± 1.34	13.85	–	11.2	–
30day	30.19	−1.03 ± 2.97	11.14	–	19.86	–	9.98	–	9.66	–
60day	28.07	–	0	–	19.99	–	13.63	–	13.91	–
120day	36.1	11.55 ± 14.72	0	–	19.62	–	4.76	–	4.31	–
360day	75.97	5.73 ± 4.39	75.97	18.04 ± 3.7	75.97	22.24 ± 6.15	75.97	−159.19 ± 19.27	75.97	−108.76 ± 15.3

According to time lag, hours were used for daily timescale and days for the other timescales. The "-" of time lag indicates the percentage of time with significant correlations less than 30% and wavelet coherency spectrum smaller than 0.5 at a specific timescale.

respectively, before the peak VPD value (Tables 2 and 3), suggesting that water supply may not meet the atmospheric demand. However, the possible water supply limitation did not significantly affect the dominant influence of solar energy on NEP and ET, which was confirmed by the influence of PAR (Fig. 5, Table S1) and Rn (Fig. 7, Table S1) on these fluxes, respectively, even after removing the effect of Ta, VPD, SW_20 cm and SW_50 cm.

4.1.2. Solar energy dominates and soil water modulates the variations of NEP and ET from days to months timescales

The significant wavelet global power spectra for NEP and ET were observed on timescales up to 180- and 16-days, respectively (Fig. 3), suggesting that significant periodic variation of ET was shorter than that of NEP, and also indicated the relatively consistent variation of ET compared with that of NEP. Yoshida et al. (2010) and Niu et al. (2019) attributed the conservative variation of ET in evergreen coniferous forests to the strong control of trees transpiration by stomatal conductance. The decoupling coefficient (range 0–1) is generally used to quantify the degree of stomatal conductance influencing ET (Jassal et al., 2009), with values close to zero representing a strong influence of stomatal conductance (Jassal et al., 2009; Ding et al., 2013). Consistent with a pine flatwood ecosystem (Bracho et al., 2008), the small monthly value of decoupling coefficient (range 0.21–0.42) in our previous studies indicated the strong influence of stomatal conductance on variations in ET at a monthly timescale (Tang et al., 2014). The NEP was also associated with GEP from days to months timescales, confirmed by the high WTC coherence between GEP and NEP, although no continuous significant effect was observed at months timescale (Fig. S6). In addition to stomatal conductance control, the photosynthesis biological processes including carboxylation processes and mesophyll activities (van Gorsel et al., 2013; Tian et al., 2020), which are sensitive to environmental factors (e.g., PAR, VPD and SW), may also influence the variation in canopy photosynthesis. Consistent with other forest ecosystems (Oishi et al., 2018; Xu et al., 2020), both the stomatal conductance and photosynthesis biological processes may contribute to a relatively large proportion of the variation in NEP compared with ET. Furthermore, the influence effect of SW on carbon and water fluxes at these timescales should not be neglected, as the negative time lag between NEP, ET and SW indicated that water supply was not consistent with the forest demand at these timescales (Tables 2 and 3). Similar to temperate forest (Oishi et al., 2018), NEP was more sensitive to the variation of SW at these timescales compared with ET in the studied forest ecosystem. This was confirmed by the higher modulating effect of soil water conditions on NEP, because there was more effect of SWs on NEP compared with ET after removing the effect of solar energy at these timescales (Table S1, Figs. S4 and S5).

Previous studies have been indicated that, in addition to direct effects, environmental factors may also indirect influence seasonal variation of forests carbon and water fluxes, through their effect on ecosystem canopy structure or leaf area (Marcolla et al., 2011; van Gorsel et al., 2013; Xu et al., 2020). In the present study, the variations of NEP and ET were primarily affected by PAR and Rn, respectively, suggesting that the variation of carbon and water fluxes from days to months timescales was associated with solar energy fluctuation and thus weather patterns, similar to a temperate deciduous forest (Hong and Kim, 2011) and a shrubland (Jia et al., 2018) – all these ecosystems were influenced by the East Asian monsoon climate. Meanwhile, based on path analysis (Fig. S7), PAR and Rn also indirectly influenced NEP and ET through their positive effect on 8-day EVI, which generally reflects the variations in canopy structure including leaf area and canopy architecture (Huete et al., 2002) and represent the capacities of plant photosynthesis and transpiration (Hong and Kim, 2011; Baldocchi et al., 2008).

4.1.3. Solar energy dominates and soil water modulates NEP and ET at an annual timescale

Both NEP and ET exhibited significant peaks of wavelet global power spectrum at an annual timescale (Fig. 3), with high values in summer (plant vigorous growth period) and low values in winter and early spring (Fig. 1). The strong fluctuation of these fluxes at this timescale was generally associated with variation of plant phenology influenced by annual solar energy and SW cycles (Zhang et al., 2011; Keenan et al., 2014). Similar to studies in forest and wetland ecosystem (Ouyang et al., 2014; Jia et al., 2018), Ta showed the strongest synchrony with NEP based on the time lag (Table 2). Keenan et al. (2014) suggested that Ta played an essential role in forest NEP at an annual timescale through its effect on plant phenology, such as leaf area index (Chen et al., 2009), leaf emergence and senescence (Jia et al., 2018), and growing season length (Baldocchi, 2008). In the studied plantation, it was showed that Ta influenced the annual variation of NEP through its effect on growing season length (Zhang et al., 2011). However, no significant effect was observed between NEP and Ta after removing the effect of SW, indicating that soil water conditions significantly modulated the effect of Ta on this carbon flux at an annual timescale.

Similar to studied semiarid (Ding et al., 2013) and arid crop ecosystems (Suyker and Verma, 2008), the Rn was the main factor affecting ET at an annual timescale in the studied plantation, even after removing the effects of Ta, VPD, SW_20 cm and SW_50 cm (Fig. 7). The less confounding effect of SW on Rn suggested that SW modulated ET less compared with NEP at an annual timescale. In addition, similar time lags (approximately 3–4 months) between NEP, ET and soil water conditions were observed at an annual timescale through correlation analysis in our previous study (Xu et al., 2017), and suggested that soil water replenished by precipitation in the first half of the year may have influenced the forest carbon and water fluxes in the second half. The similar time lag between SW and NEP or ET was also observed using a stable hydrogen isotope method in temperate deciduous forest (Zhang et al., 2018), evergreen shrub (Blok et al., 2015) and desert grass (Reichmann et al., 2013) ecosystems.

4.2. High-Ta enhances the effect of SW on NEP and ET

Absorbing deep soil water is considered as forest biological adjustment process to maintain plant photosynthesis and transpiration in response to high-Ta (Zpater et al., 2013; Tang et al., 2019; Xu et al., 2020). Using stable hydrogen isotopes, Yang et al. (2015) demonstrated that evergreen coniferous trees in the studied plantation absorbed a greater proportion of water sources from deep soil layers during a drought period through their deep root system. However, the significantly decreased NEP (68.58%) and ET (13.88%), compared with the average values during the corresponding period in the other years, demonstrated that the high-Ta exceeded the drought tolerance of this plantation although deep soil water was absorbed. The significantly decreased NEP was attributed to a greater decline in GEP (26.33%) than in RE (10.92%) during high-Ta period in the present study (Fig. S1). Consistent with decreased GEP in the present study, the EVI also decreased compared with the values for other years (Fig. S8). Our present result was inconsistent with the results for a tropical rainforest in which decreased NEP was mainly attributed to the lower RE, but maintained GEP during drought stress – attributed to deep water sources absorbed (Aguilos et al., 2018; Baldocchi et al., 2018). And the significantly decreased ET was also inconsistent with the results for temperate forests that deep soil water absorbing can maintain ET by increasing leaf area during drought period, regardless of decreased stomatal conductance (Bracho et al., 2008). Furthermore, the weak significant WTC between GEP and ET from days to months timescales (Fig. S9), indicated weak coupling between carbon and water cycles in the studied plantation, although photosynthesis and transpiration processes were associated with variations in leaf stomatal (Beer et al., 2009). Zhou et al. (2008) and Jassal et al. (2009) attributed the large decreases in GEP and thus NEP compared with ET for coniferous forest to significantly decreased carboxylation processes and mesophyll activities in drought conditions.

Consistent to the second hypothesis, at daily, monthly and annual timescales, high-Ta enhanced the effect of SW_20 cm and SW_50 cm on NEP and ET, even after the effects of PAR or Rn were removed (Tables A2 and A3). Similar to temperate deciduous (Hong and Kim, 2011), semiarid shrub (Jia et al., 2018) and pine plantation (Liu et al., 2018) ecosystems, high-Ta enhanced the effect of SW and weakened the effect of solar energy parameters (PAR or Rn) on NEP and ET, especially in 2003 when there were 25 successive days of high-Ta (Tables 1, S6 and S7). In addition, high-Ta shortened the time lag of SW_20 cm and SW_50 cm on both NEP and ET at an annual timescale, suggesting that the seasonal high-Ta effect may persist for timescales of up to a year.

4.3. Cool-Ta enhances the effect of solar energy on NEP and ET

Cool-Ta may delay plant budding (Oliveira and Peñuelas, 2004), shorten the plant growth period (Zhang et al., 2011) or damage plant leaf structure (Puglielli et al., 2017), thus influencing variation in carbon and water fluxes. Previous studies on the cool-Ta effect on NEP and ET mainly focused on temperate and boreal forests, which may have been adapted to the usually occurring low-Ta stress (Baldocchi et al., 2008; Oishi et al., 2018). The significantly decreased NEP (32.2%) was mainly due to greater decrease in GEP (33.85%) compared to RE (24.57%) in response to cool-Ta (Fig. S2). The lower GEP was also consistent with the decreased EVI in the present study during the cool-Ta period compared with the values for the other years (Fig. S8). The more decreased GEP and RE during cool-Ta period, compared with the effect of high-Ta, was likely due to the cool-Ta delaying the forest budding, and even causing physiological damage to leaves in the studied plantation (Xu et al., 2017). In addition, decreased RE can be attributed to both decreased plant root and soil microbe activities and depressed GEP, as GEP acts as a supplementary carbon substrate source for RE especially for plant respiration (Vargas et al., 2011). Furthermore, the cool-Ta period is generally associated with cloudy days in the studied plantation (Zhang et al., 2011), as well as low radiation limiting photosynthesis and low VPD limiting ET (Han et al., 2019). In contrast to the high-Ta period, during the cool-Ta period, ET was not significantly lower (10.4%, $P = 0.06$) than the value of the other years.

Partially consistent to the second hypothesis, the shorter time lag between PAR and NEP was observed at daily, monthly and even annual timescales, although no continuous significant effect was observed in response to cool-Ta, compared with the average value for the other years. In the studied plantation, Zhang et al. (2011) also indicated that the plant growth length, mainly affected by cool-Ta events, influenced the annual variation of NEP. However, the shorter time lag was only observed between Ta and ET at a daily timescale, indicating that the cool-Ta effect on NEP, but not on ET remained for a long timescale.

4.4. Implications for ecosystem models

Wavelet analysis may provide implications for modeling studies, and Wang et al. (2011) and Stoy et al. (2013) improved NEP and ET estimation by selecting model input variables at multiple timescales based on wavelet analysis. WTC results in the present study indicated that the primary affecting factors and the time lag between these factors and carbon or water flux should be considered by timescale, especially for NEP, to improve model performance. For example, considering PAR at a daily timescale and Ta at an annual timescale in ecosystem models will improve NEP estimation in the studied coniferous plantation (Table 2). In addition, the positive time lag between solar energy factors, and the negative time lag between SW and NEP or ET, from daily to annual timescales in the studied plantation suggest complex responses of carbon and water fluxes to environmental variations. Vargas et al. (2011) and Stoy et al. (2013) also suggested that the time lag can be integrated into parametric models, acting as an indirect indicator of plant biological processes.

Furthermore, the effect of high- and cool-Ta events on the influence of environmental factors on NEP or ET should also be considered as separate updating parameters in ecosystem models. For example, high-Ta enhanced the effect of SW on both NEP and ET at daily and annual timescales. However, cool-Ta enhanced the effect of PAR on NEP at daily and months timescales, and only enhanced the effect of Ta on ET at a daily timescale. Therefore, developing appropriate timescale dependence models integrated into parameters including time lag between environmental factors and carbon or water flux, and abnormal Ta events effect, is essential to improve ecosystem model performance.

5. Conclusions

The dynamics of NEP and ET, and time lags between environmental factors and these fluxes, as well as the high- and cool-Ta effects were investigated through 11 years of observation for these fluxes. The NEP and ET exhibited significant daily and annual spectrum variabilities, and NEP showed broader significant spectra than NEP, especially from days to months timescales. The NEP was nearly in phase with PAR at a daily timescale even after removing the effect of other environmental factors, but exhibited the shortest time with Ta at an annual timescale. In contrast, ET exhibited the shortest time lag and preceded Rn at both daily and annual timescales, even after removing the effect of other environmental factors. From days to months timescales, the SW_20 cm and SW_50 cm modulated more variation of NEP than ET. Both the summer high-Ta and early spring cool-Ta events proportionately decreased NEP more than ET. Summer high-Ta enhanced the effect of SW on NEP and ET at a daily, months and annual timescales. However, cool-Ta enhanced the effect of PAR on NEP from daily to months timescales, and shortened the time lag between Ta and ET only at a daily timescale. This study demonstrated that NEP and ET were more sensitive to high- than cool-Ta events, and the time lag effects of these Ta events should be considered separately to adequately acknowledge the response mechanisms of these fluxes and simulate these fluxes at long

timescales.

Declaration of Competing Interest

None.

Acknowledgements

This work was supported by the National Key Research and Development Program of China (2017YFC0503904, 2016YFC0500205), the National Natural Science Foundation of China (41977425).

Supplementary materials

Supplementary material associated with this article can be found, in the online version, at doi:10.1016/j.agrformet.2020.108310.

References

Aguilos, M., Herault, B., Burban, B., Wagner, F., Bonal, D., 2018. What drives long-term variations in carbon flux and balance in a tropical rainforest in French Guiana? Agr. Forest Meteorol. 253, 114–123.
Baldocchi, D., 2008. Breathing of the terrestrial biosphere: lessons learned from a global network of carbon dioxide flux measurement systems. Aust. J. Bot. 56 (1), 1–26.
Baldocchi, D., Chu, H.S., Reichstein, M., 2018. Inter-annual variability of net and gross ecosystem carbon fluxes: a review. Agr. Forest Meteorol. 249, 520–533.
Baldocchi, D., Kelliher, F.M., Black, T.A., Jarvis, P., 2000. Climate and vegetation controls on boreal zone energy exchange. Glob. Change Biol. 6, 69–83.
Blok, D., et al., 2015. Deepened winter snow increases stem growth and alters stem delta C-13 and delta N-15 in evergreen dwarf shrub Cassiope tetragona in high-arctic Svalbard tundra. Environ. Res. Lett. 10 (4).
Bracho, R., et al., 2008. Environmental and biological controls on water and energy exchange in Florida scrub oak and pine flatwoods ecosystems. J. Geophys. Res.-Biogeo. 113 (G2).
Chen, B.Z., et al., 2009. Seasonal controls on interannual variability in carbon dioxide exchange of a near-end-of rotation Douglas-fir stand in the Pacific Northwest, 1997-2006 Glob. Change Biol. 15 (8), 1962–1981.
Ding, R.S., Kang, S.Z., Vargas, R., Zhang, Y.Q., Hao, X.M., 2013. Multiscale spectral analysis of temporal variability in evapotranspiration over irrigated cropland in an arid region. Agr. Water Manage. 130, 79–89.
Falge, E., et al., 2001. Gap filling strategies for long term energy flux data sets. Agr. Forest Meteorol. 107 (1), 71–77.
Granier, A., et al., 2007. Evidence for soil water control on carbon and water dynamics in European forests during the extremely dry year, 2003 Agr. Forest Meteorol. 143 (1–2), 123–145.
Grinsted, A., Moore, J.C., Jevrejeva, S., 2004. Application of the cross wavelet transform and wavelet coherence to geophysical time series. Nonlinear Proc. Geoph. 11 (5–6), 561–566.
Han, J.Y., et al., 2019. Effects of sky conditions on net ecosystem productivity of a subtropical coniferous plantation vary from half-hourly to daily timescales. Sci. Total Environ. 651, 3002–3014.
Hong, J., Kim, J., 2011. Impact of the Asian monsoon climate on ecosystem carbon and water exchanges: a wavelet analysis and its ecosystem modeling implications. Glob. Change Biol. 17 (5), 1900–1916.
Hu, Z.M., et al., 2018. Shifts in the dynamics of productivity signal ecosystem state transitions at the biome-scale. Ecol. Lett. 21 (10), 1457–1466.
Jassal, R.S., Black, T.A., Spittlehouse, D.L., Brummer, C., Nesic, Z., 2009. Evapotranspiration and water use efficiency in different-aged Pacific Northwest Douglas-fir stands. Agr. Forest Meteorol. 149 (6–7), 1168–1178.
Jia, X., et al., 2018. Multi-scale dynamics and environmental controls on net ecosystem CO2 exchange over a temperate semiarid shrubland. Agr. Forest Meteorol. 259, 250–259.
Keenan, T.F., et al., 2014. Net carbon uptake has increased through warming-induced changes in temperate forest phenology. Nat. Clim. Change 4 (7), 598–604.
Kelliher, F.M., Leuning, R., Raupach, M.R., Schulze, E.D., 1995. Maximum conductances for evaporation from global vegetation types. Agr. Forest Meteorol. 73 (1–2), 1–16.
Koebsch, F., Jurasinski, G., Koch, M., Hofmann, J., Glatzel, S., 2015. Controls for multi-scale temporal variation in ecosystem methane exchange during the growing season of a permanently inundated fen. Agr. Forest Meteorol. 204, 94–105.
Liu, X., et al., 2018. Drought and thinning have limited impacts on evapotranspiration in a managed pine plantation on the southeastern United States coastal plain. Agr. Forest Meteorol. 262, 14–23.
Marcolla, B., et al., 2011. Climatic controls and ecosystem responses drive the inter-annual variability of the net ecosystem exchange of an alpine meadow. Agr. Forest Meteorol. 151 (9), 1233–1243.
Mi, N., et al., 2009. Use of ecosystem flux data and a simulation model to examine seasonal drought effects on a subtropical coniferous forest. Asia-Pac. J. Atmos. Sci. 45 (2), 207–220.
Moore, C.J., 1986. Frequency response corrections for eddy correlation systems. Bound-Lay Meteorol. 37, 17–35.
Niu, Z.G., et al., 2019. An increasing trend in the ratio of transpiration to total terrestrial evapotranspiration in China from 1982 to 2015 caused by greening and warming. Agr. Forest Meteorol. 279.
Oishi, A.C., et al., 2018. Warmer temperatures reduce net carbon uptake, but do not affect water use, in a mature southern Appalachian forest. Agr. Forest Meteorol. 252, 269–282.
Oliveira, G., Penuelas, J., 2004. Effects of winter cold stress on photosynthesis and photochemical efficiency of PSII of the Mediterranean Cistus albidus L. and Quercus ilex L. Plant. Ecol. 175 (2), 179–191.
Ouyang, Z.T., et al., 2014. Disentangling the confounding effects of PAR and air temperature on net ecosystem exchange at multiple time scales. Ecol. Complex 19, 46–58.
Piao, S.L., et al., 2010. Forest annual carbon cost: a global-scale analysis of autotrophic respiration. Ecology 91 (3), 652–661.
Puglielli, G., Spoletini, A., Fabrini, G., Gratani, L., 2017. Temperature responsiveness of seedlings maximum relative growth rate in three Mediterranean Cistus species. J. Plant Ecol. 10 (2), 331–339.
Reichmann, L.G., Sala, O.E., D.P.C., Peters, 2013. Precipitation legacies in desert grassland primary production occur through previous-year tiller density. Ecology 94 (2), 435–443.
Reichstein, M., et al., 2005. On the separation of net ecosystem exchange into assimilation and ecosystem respiration: review and improved algorithm. Glob. Change Biol. 11 (9), 1424–1439.
Silvertown, J., Araya, Y., Gowing, D., 2015. Hydrological niches in terrestrial plant communities: a review. J. Ecol. 103 (1), 93–108.
Stoy, P.C., et al., 2013. Evaluating the agreement between measurements and models of net ecosystem exchange at different times and timescales using wavelet coherence: an example using data from the North American Carbon Program Site-Level Interim Synthesis. Biogeosciences 10 (11), 6893–6909.
Suyker, A.E., Verma, S.B., 2008. Interannual water vapor and energy exchange in an irrigated maize-based agroecosystem. Agr. Forest Meteorol. 148 (3), 417–427.
Tang, Y.K., et al., 2016. Variation of carbon use efficiency over ten years in a subtropical coniferous plantation in southeast China. Ecol. Eng. 97, 196–206.
Tang, Y.K., Wen, X.F., Sun, X.M., Zhang, X.Y., Wang, H.M., 2014. The limiting effect of deep soil water on evapotranspiration of a subtropical coniferous plantation subjected to seasonal drought. Adv. Atmos. Sci. 31 (2), 385–395.
Tang, Y.K., Wu, X., Chen, C., Jia, C., Chen, Y.M., 2019. Water source partitioning and nitrogen facilitation promote coexistence of nitrogen-fixing and neighbor species in mixed plantations in the semiarid Loess Plateau. Plant Soil. 445 (1–2), 289–305.
Tian, X.L., et al., 2020. Extending the range of applicability of the semi-empirical ecosystem flux model PRELES for varying forest types and climate. Glob. Change Biol.
van Gorsel, E., et al., 2013. Primary and secondary effects of climate variability on net ecosystem carbon exchange in an evergreen Eucalyptus forest. Agr. Forest Meteorol. 182, 248–256.
Vargas, R., et al., 2011. On the multi-temporal correlation between photosynthesis and soil CO2 efflux: reconciling lags and observations. New Phytol. 191 (4), 1006–1017.
Wang, Y.P., et al., 2011. Diagnosing errors in a land surface model (CABLE) in the time and frequency domains. J. Geophys. Res.-Biogeo. 116.
Webb, E.K., Pearman, G.I., Leuning, R., 1980. Correction of flux measurements for density effects due to heat and water-wapor transfer. Q. J. R. Meteological Soc. 106 (447), 85–100.
Wen, X.F., Wang, H.M., Wang, J.L., Yu, G.R., Sun, X.M., 2010. Ecosystem carbon exchanges of a subtropical evergreen coniferous plantation subjected to seasonal drought, 2003-2007. Biogeosciences 7 (1), 357–369.
Wilczak, J.M., Oncley, S.P., Stage, S.A., 2001. Sonic anemometer tilt correction algorithms. Bound-Lay Meteorol. 99 (1), 127–150.
Wilson, K.B., et al., 2002. Energy partitioning between latent and sensible heat flux during the warm season at FLUXNET sites. Water Resour. Res. 38 (12).
Xu, H., et al., 2020. Environmental and canopy stomatal control on ecosystem water use efficiency in a riparian poplar plantation. Agr. Forest Meteorol. 287.
Xu, M.J., et al., 2017. The full annual carbon balance of a subtropical coniferous plantation is highly sensitive to autumn precipitation. Sci. Rep.-Uk 7.
Yang, B., Wen, X.F., Sun, X.M., 2015. Seasonal variations in depth of water uptake for a subtropical coniferous plantation subjected to drought in an East Asian monsoon region. Agr. Forest Meteorol. 201, 218–228.
Yoshida, M., Ohta, T., Kotani, A., Maximov, T., 2010. Environmental factors controlling forest evapotranspiration and surface conductance on a multi-temporal scale in growing seasons of a Siberian larch forest. J. Hydrol. 395 (3–4), 180–189.
Zhang, H., Wen, X.F., 2015. Flux footprint climatology estimated by three analytical models over a subtropical coniferous plantation in Southeast China. J. Meteorol. Res.-Prc. 29 (4), 654–666.
Zhang, W.J., et al., 2011. Underestimated effects of low temperature during early growing season on carbon sequestration of a subtropical coniferous plantation. Biogeosciences 8 (6), 1667–1678.
Zhang, X.B., Hegerl, G., Zwiers, F.W., Kenyon, J., 2005. Avoiding inhomogeneity in percentile-based indices of temperature extremes. J. Climate 18 (11), 1641–1651.
Zhang, Y.J., et al., 2014. Climate-driven global changes in carbon use efficiency. Glob. Ecol. Biogeogr. 23 (2), 144–155.
Zhang, Y.P., Jiang, Y., Wang, B., Jiao, L., Wang, M.C., 2018. Seasonal water use by Larix principis-rupprechtii in an alpine habitat. Forest Ecol. Manag. 409, 47–55.
Zhou, X.H., Weng, E.S., Luo, Y.Q., 2008. Modeling patterns of nonlinearity in ecosystem responses to temperature, CO_2, and precipitation changes. Ecol. Appl. 18 (2), 453–466.